JOURNAL DE PHYSIQUE
Colloque C2, supplément au n° 6, Tome 48, juin 1987

NUCLEAR GIANT RESONANCES IN COORDINATE SPACE - A SEMICLASSICAL DENSITY FUNCTIONAL APPROACH [1]

P. GLEISSL, M. BRACK, J. MEYER[2] and Ph. QUENTIN[3]

Institut für Theoretische Physik, Universität Regensburg, D-8400 Regensburg, F.R.G.

Résumé: Dans le cadre d'une description semiclassique de résonnances géantes nucléaires (GR) en utilisant la force SkM* et les fonctionnelles ETF complètes à l'ordre 4 en $\hbar$, nous présentons des modes propres monopolaires (0^+) isoscalaires ($I=0$) et isovectorielles ($I=1$) en bon accord avec l'expérience, ainsi que la variation de quelques énergies GR typiques en fonction de la température.

Abstract: We discuss the semiclassical description of nuclear giant resonances (GR) using a realistic Skyrme force (SkM*) and complete ETF density functionals. We present monopole (0^+) eigenmodes of isoscalar ($I=0$) and isovector ($I=1$) type, which are in good agreement with experiment, and the corresponding m_1 and m_3 sum rules. We also present the temperature dependence of some typical GR energies (0^+,I=0,1; 1^-,I=1; 2^+,I=0) in ^{208}Pb.

The density variational method using Skyrme type effective forces and semiclassical ETF (extended Thomas-Fermi) density functionals has been very successful for the calculation of average static properties of nuclei /1,2/. This approach has been shown /1/ to yield precisely the average part of selfconsistent microscopical HF (Hartree-Fock) results, leaving out the shell effects. (Similar results were recently obtained also for the Gogny finite-range force D1 /3/.) Shell effects in the nuclear binding and deformation energies can be recovered perturbatively to a high degree of accuracy /1,4/ by exploiting the Strutinsky energy theorem /5,6/. The density functional approach becomes particularly gratifying for highly excited nuclear systems: At excitation energies corresponding to temperatures of $kT \simeq 2.5 - 3$ MeV and higher, shell effects vanish and the ETF density functionals become exact /7,8/, thus yielding the same results as fully microscopic HF calculations.

When applying these ideas to the description of dynamic nuclear processes, one is at first handicapped by the fact that the ETF functionals do not apply, in general, to situations where the density is time dependent, except for the case of slow adiabatic motion. Although some formal progress has been achieved in the foundation of time-dependent density functional theory /9/, ready-to-use functionals are not yet at hand.

In the study of giant resonances (GR) it has been realized /10/ that dynamical deformations of the Fermi sphere in momentum space, which are missed when using the static ETF functionals /11/, give important contributions to the restoring forces of some modes (e.g. all isoscalar electric multipole modes with $L \geq 2$). These effects, which in an infinite system lead to Landau zero-sound excitations, have been incorporated to various degrees of sophistication in the so-called fluid-dynamical approach and its variations /10,12-17/, leading to good agreement with the results of RPA calculations and - to the extent that this is the case for the RPA results - with experiment. In many of these calculations, however, very schematic energy density functionals ignoring Coulomb and spin-orbit forces were used; the higher-order gradient corrections to the kinetic energy, known to be important to reproduce correctly static nuclear surface and deformation properties /1/, were omitted, too.

[1] Work partially supported by the German-French scientific exchange program "PROCOPE"

[2] Permanent address : I.P.N. (and IN2P3), Université de Lyon-I, F-69622 Villeurbanne Cedex, France

[3] Permanent address : Laboratoire de Physique Théorique, Université de Bordeaux-I, F-33170 Gradignan, France

In the present paper we want to report on a related approach which takes full advantage of the complete ETF functionals (also at finite temperatures) and realistic Skyrme interactions in calculating eigenmodes and sum rules corresponding to various giant resonances /18-20/. (For similar calculations with approximate ETF functionals see also refs. /21-23/.) As is well-known, there exist theorems /24-26/ relating RPA sum rules to HF ground state expectation values. In particular, one has (see ref./26/ for details)

$$m_3(Q) = -\frac{1}{2}\langle 0|[\hat{S},[\hat{H},\hat{S}]]|0\rangle \quad , \quad \hat{S} = [\hat{H},Q] \quad , \tag{1}$$

$$m_1(Q) = \frac{1}{2}\langle 0|[Q,[\hat{H},Q]]|0\rangle \quad , \tag{2}$$

$$m_{-1}(Q) = \frac{1}{2}\left[\frac{d^2}{d\lambda^2}\langle\lambda|\hat{H}|\lambda\rangle\right]_{\lambda=0} = \frac{1}{2}\left[\frac{d}{d\lambda}\langle\lambda|Q|\lambda\rangle\right]_{\lambda=0} \quad . \tag{3}$$

Hereby $m_k(Q)$ is the k-th moment of the strength function corresponding to a chosen excitation operator Q; $|\lambda\rangle$ is the solution of the static constrained HF problem $\delta\langle \hat{H} - \lambda Q\rangle = 0$ with λ as a Lagrange multiplier. $\hat{H}$ is the total Hamiltonian of the system including the effective (e.g. Skyrme) nucleon-nucleon interaction. The virtue of eqs. (1)-(3) is that the expressions on the r.h.s. are static HF expectation values which can be evaluated semiclassically with the static ETF functionals (at the possible cost of missing shell effects which, however, are very small for the giant resonance energies, see Fig.1 below); hereby it is essential that the commutators in eq. (1) be evaluated quantum-mechanically. The knowledge of the three moments (1)-(3) allows one to estimate the mean energy $\bar{E}$ of a giant resonance peak by the inequality

$$E_1 \leq \bar{E} \leq E_3 \quad , \quad E_k = \sqrt{m_k/m_{k-1}} \quad , \tag{4}$$

and its width Γ for which $\sqrt{E_3^2 - E_1^2}/2$ is an upper bound.

One-body excitation operators Q which commute with the two-body force in $\hat{H}$ (e.g. local and velocity-independent isoscalar operators in connection with Skyrme forces) can be understood as generators of collective scaling-type deformations α by means of unitary transformations of the HF ground state:

$$|\alpha\rangle = e^{-\alpha\hat{S}}|0\rangle \quad , \quad \hat{S} = [\hat{T},Q] = \frac{1}{2}\vec{\nabla}\cdot\vec{u} + \vec{u}\cdot\vec{\nabla} \quad , \quad \vec{u} = -\frac{\hbar^2}{m}\cdot\vec{\nabla}Q. \tag{5}$$

Here $\vec{u}$ is recognized as a displacement field defining the velocity field $\vec{v} = \dot{\alpha}(t)\,\vec{u}$ which satisfies the continuity equation $d\rho/dt + \vec{\nabla}\cdot(\rho\vec{v}) = 0$, where $\rho(\vec{r},\alpha(t))$ is the scaled HF ground state density. The moment m_1 is then easily shown to be proportional to the hydrodynamical inertial parameter B_α:

$$m_1(Q) = \frac{m}{2\hbar^2}\int d^3r\, \vec{u}^2\rho = \frac{1}{2\hbar^2}B_\alpha \quad , \tag{6}$$

and m_3 is found to be one-half of the harmonic oscillator spring constant C_α of the scaled HF energy:

$$m_3(Q) = \frac{1}{2}\left[\frac{d^2}{d\alpha^2}\langle\alpha|\hat{H}|\alpha\rangle\right]_{\alpha=0} = \frac{1}{2}C_\alpha \quad . \tag{7}$$

Thus, the energy E_3 in (4) is equal to the (first) vibrational excitation energy of the collective scaling Hamiltonian

$$H_{coll}(\alpha) = \frac{1}{2}B_\alpha\dot{\alpha}^2 + \langle\alpha|\hat{H}|\alpha\rangle \tag{8}$$

in the harmonic approximation:

$$E_3 = \sqrt{m_3/m_1} = \hbar\sqrt{C_\alpha/B_\alpha} = \hbar\omega_\alpha \quad . \tag{9}$$

Care should be taken introducing the static semiclassical functionals after taking the derivative $d^2/d\alpha^2$ in eq.(7); interchanging this order would lead to the hydrodynamical (and thus often the wrong) spring constants C_α.

The scaling approach can be generalized to a set of coupled modes α_i (i=1,2,...M)

generated by M operators Q_i /18,20,27,28/. The problem then consists in finding the eigenfrequencies ω_n of the collective Hamiltonian

$$H_{coll} = \frac{1}{2}\sum_{i,j=1}^{M} B_{ij}\,\dot{\alpha}_i\dot{\alpha}_j + \frac{1}{2}\sum_{i,j=1}^{M} C_{ij}\,\alpha_i\alpha_j + E_{HF} \tag{10}$$

by solving the matrix equation

$$(C - \omega_n^2 B)\,\vec{X}_n = 0 \qquad (n=1,2,\ldots M) \tag{11}$$

with

$$B_{ij} = 2\hbar^2 m_1(i,j) = \hbar^2 \langle 0 \mid [Q_i,[\hat{H},Q_j]] \mid 0 \rangle, \tag{12}$$

$$C_{ij} = 2m_3(i,j) = -\langle 0 \mid [\hat{S}_i,[\hat{H},\hat{S}_j]] \mid 0 \rangle. \tag{13}$$

Exploiting the generalized Thouless theorem /26/ for the mixed moments

$$m_k(i,j) = \sum_{n>0} (\tilde{E}_n - \tilde{E}_0)^k \langle \tilde{0} \mid Q_i \mid \tilde{n} \rangle \langle \tilde{n} \mid Q_j \mid \tilde{0} \rangle, \tag{14}$$

where $|\tilde{n}\rangle$ and $\tilde{E}_n$ are the RPA states and energies, respectively, one can easily show that the M eigenmodes defined by eq.(11) exhaust the m_1 and m_3 RPA sum rules eqs.(1), (2) for any operator Q which can be expanded in terms of the finite basis of the Q_i. (In practice it may be easier - and sometimes more physical - not to start from a guess of the operators Q_i but rather to introduce some reasonably chosen collective variables α_i and to reconstruct the $\vec{u}_i$ and Q_i by solving the corresponding continuity equations /18,20,28/.)

A difference of the above approach to the fluid-dynamical one (e.g. refs./14,16/) is that in the latter one automatically is led to an infinite set of eigenmodes. This is mathematically satisfying, but has the consequence that many (i.e. almost all) of the eigenmodes lie at energies where the model does not apply (e.g. above the pion threshold) and thus some of the collective strength may appear in unphysical states.

The treatment of isovector (I=1) giant resonances and operators Q is more difficult. The non-zero commutators of Q with the two-body force in this case gives additionalcontributions to the moments m_1 and m_3 which are usually expressed through the so-called 'acceleration factors' κ_k. Although these may in principle be incorporated in the scaling approach /12/, this becomes rather involved in particular when evaluating $m_3(i,j)$ in a multidimensional treatment.

In the following we shall illustrate the above ideas with a few examples. A more exhaustive presentation of our calculations is in preparation /20/. We used throughout the Skyrme force SkM* /1,29/ and the full ETF functionals up to fourth order in $\hbar$ /1,7,8/; so far only spherical nuclei were considered.

In Fig. 1 we demonstrate the smallness of the shell effects in the energies E_3 (9) evaluated for some giant resonances as functions of the particle number A. The operators Q chosen for calculating m_1 and m_3 are

$$Q = \sum_{i=1}^{A} r_i^2 \qquad \text{for } 0^+,\ I=0 \quad \text{(isoscalar monopole)}, \tag{15}$$

$$Q = \sum_{i=1}^{A} r_i^2\,\tau_3(i) \qquad \text{for } 0^+,\ I=1 \quad \text{(isovector monopole)}, \tag{16}$$

$$Q = \sum_{i=1}^{A} r_i^2\,P_2(\cos\theta_i) \qquad \text{for } 2^+,\ I=0 \quad \text{(isoscalar quadrupole)}. \tag{17}$$

In the isovector monopole case, the acceleration factors were neglected (see, however, Tab. 2 below). The solid lines show the semiclassical values of E_3, evaluated with the static ETF functionals for spherical nuclei along a smooth fit to the β-stability valley in the (N,Z)-plane. They are seen to give an excellent approximation to the microscopic HF values which are shown by crosses for a sample of corresponding nuclei.(Their shapes were constrained to be spherical in the HF calculations.) We should mention at this place that this close agreement between HF and semiclassical results is not found for the energies E_1 in all cases; the moments m_{-1} in some modes are much more sensitive to shell effects (see Tab. 2 and the discussion below).

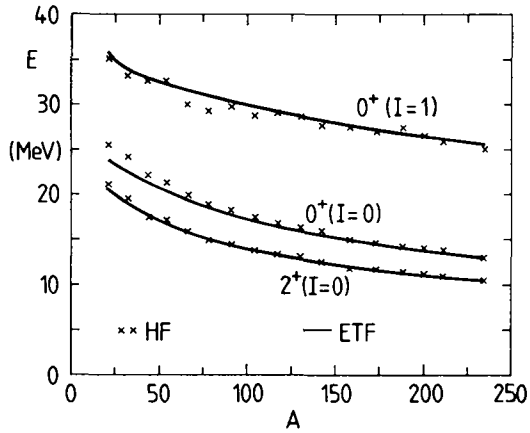

Fig. 1:
GR energies $E_3=\sqrt{m_3/m_1}$ (without acceleration factors for the I=1 monopole) versus nucleon number A.
Crosses: HF values,
solid line: ETF values for nuclei along the β-stability valley in the (N,Z)-plane.
Note the small differences which are essentially due to the shell effects. (Minor smooth differences in the light nuclei may also stem from an insufficient parametrization of the nucleon densities in the ETF calculation.)
The Skyrme force SkM* was used in both calculations.

	I=0				I=1			
	$\hbar\omega_i$ [MeV]	E_{exp} [MeV]	%(m_1)	%(m_3)	$\hbar\omega_i$ [MeV]	E_{exp} [MeV]	%(m_1)	%(m_3)
^{40}Ca	35.5		3.66	9.79	44.1		19.2	34.6
	21.0		96.34	90.21	29.5	31.1±2.2	80.8	65.4
^{60}Ni	33.9		1.23	3.59	42.6		12.9	23.6
	19.6	19.8±0.5	98.77	96.41	29.5	30.6±2.3	87.1	76.4
^{90}Zr	32.1		0.25	0.82	40.8		7.8	14.6
	17.7	16.9±0.9	99.75	99.18	28.8	28.5±2.6	92.2	85.4
^{120}Sn	30.2		0.05	0.17	39.5		5.0	9.5
	16.2	15.8±1.0	99.95	99.83	27.9	26.1±2.4	95.0	90.5
^{140}Ce	29.6		0.01	0.04	38.8		3.8	7.2
	15.4	14.8±0.6	99.99	99.96	27.5	28.0±2.6	96.2	92.8
^{208}Pb	27.5		0.05	0.21	37.3		1.5	3.1
	13.5	13.7±0.5	99.95	99.79	26.0	25.5±3.0	98.5	96.9

Tab. 1:
Eigenmode energies $\hbar\omega_i$ (i=1,2) of coupled bulk density and surface stiffness monopole (0^+) vibrations obtained semiclassically for 6 spherical nuclei with the SkM* force. The experimental GMR peak energies are taken from a compilation in ref. /30/ for the isoscalar (I=0) and from ref. /31/ for the isovector (I=1) case. Also shown are the percentages of the m_1 and the m_3 sum rules for the excitation operators eqs. (15,19). The acceleration factors were neglected in the I=1 case.

The idea of the generalized scaling model with coupled collective modes was applied to the giant monopole resonances (GMR, "breathing modes") in refs. /18,20,28/. The ground-state densities of neutrons and protons were parametrized by Fermi functions:

$$\rho_q(r) = \rho_{oq} \cdot \left[1 + \exp\{(r-R_q)/\alpha_q\}\right]^{-\gamma_q}. \quad (q=n,p) \qquad (18)$$

The bulk densities ρ_{oq} and the surface diffuseness parameters α_q were taken as collective variables oscillating in time (the radii R_q being adjusted such as to keep

the nucleon numbers N and Z constant; the γ_q are kept constant at the g.s. values). For isoscalar (I=0) vibrations one imposes $\rho_{on}(t)/\rho_{on}(0) = \rho_{op}(t)/\rho_{op}(0)$, for isovector vibrations (I=1) $Z\rho_{on}(t)/\rho_{on}(0) = -N\rho_{op}(t)/\rho_{op}(0)$, and analogously for the parameters $\alpha_q(t)$. Solving eq. (11) gives two eigenmodes in each case. The lower modes are dominated by the bulk density oscillation and can be identified with the experimentally observed GMR peak energies, whereas the higher ones are dominated by the surface oscillation and have not yet been identified experimentally. (Their transition densities typically have two nodes in the surface region /18,20/ and are very similar to the ones of higher lying 0^+ states found also in RPA calculations /D.Gogny, private communication/.)

In Tab. 1 we show the eigenmode energies $\hbar\omega_i$ (i=1,2) obtained for some spherical nuclei. The isoscalar results (I=0) correspond to those of ref. /18/, but using $\gamma_q \neq 1$ for the g.s. densities (18) in the variational ETF calculation. As already observed in ref. /18/, the agreement with the experimental GMR peak energies (given in Tab. 1 with error bars) is excellent. A similarly good agreement is also found /20/ for the lower isovector modes with the newly measured 0^+, I=1 energies /31/. This agreement is, however, accidental since the acceleration factors (i.e. the commutators of the operators Q_i with the Skyrme force) have been neglected here. Their influence will be discussed in connection with Tab. 2 below. We also show in Tab. 1 the percentages of the m_1 and m_3 sum rules for the operator eq. (15) in the I=0 and the operator

$$Q = \frac{A}{4}\sum_{i=1}^{A}\left[\left(\frac{1}{Z} - \frac{1}{N}\right) + \left(\frac{1}{Z} + \frac{1}{N}\right)\cdot\tau_3(i)\right] r_i^2 \qquad (0^+, I=1) \qquad (19)$$

in the I=1 case. (This operator is more correct than that of eq. (16) which leads to a small I=0 component in nuclei with N≠Z.) The distribution of strength over the two modes reflects the importance of the surface component of the oscillations, which is especially pronounced for light nuclei in the isovector modes, due to a larger coupling of the two modes through the off-diagonal matrix elements B_{12} and C_{12}. The result of this coupling is to push the eigenfrequencies ω_i further apart from their uncoupled positions $\sqrt{C_{ii}/B_{ii}}$. This is demonstrated also in Fig. 2 for the isovector GMR. The dots with error bars and the crosses connected by a dashed line show the experimental GMR peak energies and the lower eigenenergies $\hbar\omega_1$, respectively, from Tab. 1.

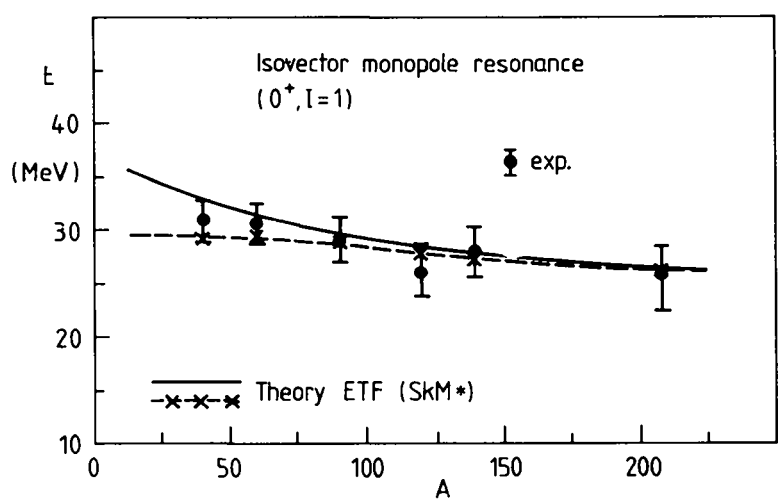

Fig. 2:

Isovector GMR energies obtained in the generalized scaling model (without acceleration factors). Solid line: Energy E_3 with operator eq. (19). Crosses connected by dashed line: lowest eigenenergy $\hbar\omega_1$ of two coupled modes (see text). ETF functionals and SkM* force used. Experimental points from Los Alamos ($\pi^{\pm}$,π^0) measurements /31/.

The solid line results from a one-dimensional semiclassical scaling calculation and corresponds to the energy E_3 (without acceleration factors) with the operator Q eq. (19). This scaling implies a fixed ratio between surface and bulk density vibrations (ratio -1/3 between relative changes in α_q and ρ_{0q}, see ref./18/). Letting the surface vary freely in the two-dimensional calculation lowers the energies $\hbar\omega_1$, especially for the lighter nuclei, leading to a somewhat better agreement of their A-dependence with experiment. It would be interesting if experiments for the I=1 GMR could be made also for nuclei lighter than ^{40}Ca, since there the predicted differences between the results with one and two collective variables would exceed the expected error bars of the peak energies. The importance of the surface diffuseness degree of freedom for the 0^+, I=1 mode has also been recognized in ref. /32/.

	κ_1		m_{-1} [Mev^{-1}fm^4]		E_1 [MeV]	
	ETF	HF	ETF	HF	ETF	HF
^{40}Ca	0.251	0.242	38.7	49.4	34.7	30.7
^{90}Zr	0.295	0.297	163	185	32.8	30.7
^{208}Pb	0.333	0.332	872	986	29.0	27.2

Tab. 2:

Acceleration factors κ_1, sum rules m_{-1} and energies E_1 for the isovector monopole operator Q eq. (19), calculated for three spherical nuclei with the SkM* force. Both semiclassical (ETF) and Hartree-Fock (HF) results are given.

In order to check the importance of the acceleration factors neglected so far, we have calculated the full moment m_1 including the Skyrme force for the isovector monopole operator Q eq. (19). Evaluating the commutators in eq. (2) gives

$$m_1 = \frac{1}{2}\langle 0 \,|[Q,[\hat{T},Q]]\,| 0\rangle (1+\kappa_1) =$$

$$= \frac{A^2}{4}\left\{\frac{2\hbar^2}{m}\left(\frac{1}{Z}\langle r^2\rangle_p + \frac{1}{N}\langle r^2\rangle_n\right) + \left(\frac{1}{Z}+\frac{1}{N}\right)^2\left[t_1\left(1+\frac{x_1}{2}\right) + t_2\left(1+\frac{x_2}{2}\right)\right]\int r^2\rho_n\rho_p d^3r\right\}, \qquad (20)$$

where t_i und x_i are Skyrme force parameters. The values of the acceleration factor κ_1 defined in eq. (20) are given in Table 2 for three spherical nuclei. They were evaluated both microscopically (HF) and semiclassically (ETF using the density parametrisation eq. (18)). The differences are ~4% for Ca and less than 1% for medium and heavy nuclei. We also give in Tab. 2 the moments m_{-1} and energies E_1 from which the m_1 can easily be gained, see eq. (4). The m_1 values differ by less than 1% between ETF and HF in all nuclei; thus, the ~3% difference in the mean square radii of Ca /1/ mostly cancels that in the κ_1 values.

Much larger differences between HF and ETF values are, however, found for the static polarisabilities m_{-1} and thus also for the energies E_1. These differences reveal a rather strong shell effect in the polarisabilities m_{-1}, amounting to ~22% in Ca and ~12% in the medium and heavy nuclei. It is not too surprising that the response to a static external constraining field, in which the single particle states have time to readjust their orbits, is sensitive to shell effects. An even more drastic example would be the quadrupole polarisabilities (i.e. the m_{-1} with Q eq.(17)) of heavy nuclei, which are well-known to be dominated by the shell effects (the semiclassical or liquid drop part only contributing a fraction, see refs. /5,6/).

HF calculations for the isovector GMR were reported also in ref. /33/. These authors used, however, the excitation operator Q eq. (16). In ^{40}Ca, where there is no difference to the one in eq. (19) which we have used, our HF results for m_{-1} and E_1 agree exactly. In N≠Z nuclei they obtain spurious isoscalar (I=0) admixtures amounting e.g. for ^{208}Pb to -2.3 MeV in E_1.

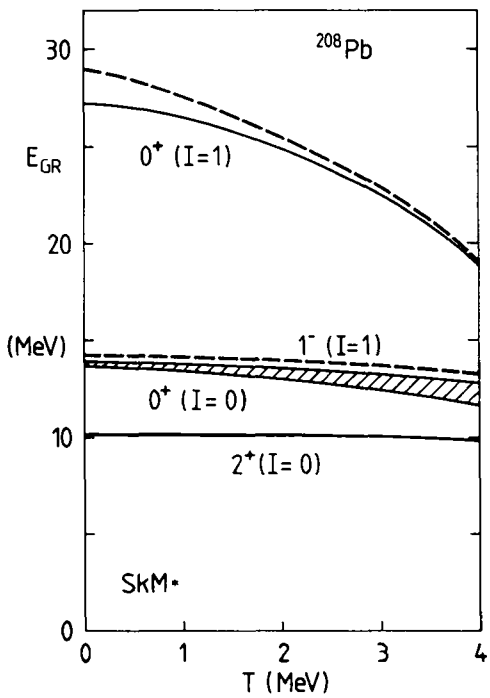

Fig. 3:

Nuclear giant resonance energies versus temperature T.
Solid lines: HF results, dashed lines: semiclassical ETF results.

2^+ (I=0): energy E_3 with operator (17).

0^+ (I=0): upper line: E_3, lower line: E_1 both with operator(15). The difference (=shaded area) is a measure for the width Γ.

1^- (I=1): energy E_1 including κ_1 (see ref. /19/ for details).

0^+ (I=1): energy E_1 (including κ_1) with operator (19). Note the decrease of the shell effect with increasing temperature.

The SkM* force was used in all cases.

The HF values for E_1 in Tab. 2 are seen to be in reasonable agreement with the experimental peak energies in Tab. 1, taking the rather large error bars of the latter into account. Note that a similar agreement would be obtained also for the ETF values of E_1 if the κ_1 factors were neglected; this would, however, be due to a fortuitous cancellation of two completely different errors, namely the omission of κ_1 and of the shell effects in m_{-1}.

We finally want to comment briefly on the temperature dependence of the calculated nuclear giant resonance energies. (See also the following paper /23/ where a more detailed discussion of the finite temperature approach is found.) We limit ourselves here to temperatures up to $T \sim 4$ MeV (k=1) where the continuum effects play a minor role and the density parametrisation eq. (18) is sufficient.

In Fig. 3 we present the energies of various modes as functions of the temperature (see the explanations in the figure caption). They are seen to vary very little (or not at all in the 2^+ mode), except for the isovector monopole case (0^+, I=1). Here we give the energy E_1 using the operator Q eq. (19) and including the κ_1 factor both in HF (solid line) and in ETF (dashed line) approximation. The shell effect discussed above for T=0 is seen to decrease with increasing temperature and to practically vanish for $T \gtrsim 3$ MeV, as expected. We do not believe that the isovector GMR is likely to be measured for excited nuclei, but we show these results as another nice example for the disappearance of the shell effects at $T \gtrsim 3$ MeV enabling the use of the semiclassical approximation. We refer to ref. /20/ for a more detailed discussion of the finite temperature results and of the dipole (1^-), quadrupole (2^+) and octupole (3^-) modes.

We acknowledge stimulating discussions with E.Lipparini, J. and J.P. da Providência and S.Stringari. Two of us (P.G. and M.B.) acknowledge the warm hospitality of the Institut de Physique Nucléaire at the Université de Lyon, where part of this work was achieved.

References:

1. M. Brack, C. Guet and H.-B. Håkansson, Phys. Reports 123 (1985) 275.
2. J. Treiner and H. Krivine, Ann. of Phys. 170 (1986) 406.
3. J. Meyer et al., Phys. Lett. 172B (1986) 122.
4. F. Tondeur, A. K. Dutta, J. M. Pearson and R. Behrman, Nucl. Phys. A, to be published.
5. V. M. Strutinsky, Nucl. Phys. A122 (1968) 1.
6. M. Brack and P. Quentin, Nucl. Phys. A361 (1981) 35.
7. J. Bartel, M. Brack and M. Durand, Nucl. Phys. A445 (1985) 263.
8. M. Brack and J. Bartel, Proc. of IVth International Symposium on Recent Progress in Many Body Theories, San Francisco, 1985, eds. P. Siemens and R. Smith (Springer, New York) to be published.
9. H. Kohl, these Proceedings.
10. G. F. Bertsch, Nucl. Phys. A249 (1975) 253.
11. B. K. Jennings, Phys. Lett. 96B (1980) 1.
12. S. Stringari, Nucl. Phys. A279 (1977) 454; Ann. Phys. 151 (1983) 35.
13. C. Y. Wong and J. A. MacDonald, Phys. Rev. C16 (1977) 1196.
14. H. Sagawa and G. Holzwarth, Progr. Theor. Phys. 59 (1978) 1213; G. Holzwarth and G. Eckardt, Z. Phys. A284 (1978) 291.
15. J. R. Nix and A. J. Sierk, Phys. Rev. C21 (1980) 396.
16. J. P. da Providência and G. Holzwarth, Nucl. Phys. A398 (1983) 59, A439 (1985) 477; J. P. da Providência, Ph. D. Thesis, Siegen University, 1982.
17. V. M. Strutinsky, A. Magner and V. Denisov, Z. Phys. A315 (1984) 301; A. Magner and V. M. Strutinsky, Z. Phys. A322 (1985) 633 and preprint 1986.
18. M. Brack and W. Stocker, Nucl. Phys. A406 (1983) 413.
19. J. Meyer, P. Quentin and M. Brack, Phys. Lett. 133B (1983) 279; see also Proc.of 7th Biennale de Physique Nucléaire, Aussois 1983, Report LYCEN 8302 (Université de Lyon, 1983), p. C131.
20. P. Gleißl, Diploma Thesis, Regensburg University, 1985; P. Gleißl, M. Brack, J. Meyer and P. Quentin, to be published.
21. M. Barranco et al., Phys. Lett. 154B (1985) 96, and references quoted therein.
22. M. Barranco, A. Polls and J. Martorell, Nucl. Phys. A444 (1985) 445.
23. E. Suraud et al., these Proceedings.
24. D. J. Thouless, Nucl. Phys. 22 (1961) 78.
25. E. R. Marshalek and J. da Providencia, Phys. Rev. C7 (1973) 2281.
26. O. Bohigas, A. M. Lane and J. Martorell, Phys. Reports 51 (1979) 267.
27. Y. Abgrall et al., Nucl. Phys. A346 (1980) 431.
28. A. S. Jensen and S. M. Larsen, Phys. Scripta 24 (1981) 534.
29. J. Bartel et al., Nucl. Phys. A386 (1982) 79.
30. J. Treiner, H. Krivine, O. Bohigas and J. Martorell, Nucl. Phys. A371 (1981) 253.
31. A. Erell et al., Phys. Rev. Lett. 52 (1984) 2134.
32. E. Lipparini, these Proceedings, and private communication.
33. M. Casas, J. Martorell and J. Gomez, Phys. Lett. 152B (1985) 6.